# Broadband Lasing Characteristics of a Chirped InAs/InP Quantum-Dash Laser

E. Alkhazraji, M. Talal A. Khan and M. Z. M. Khan
*Electrical Engineering Department, King Fahd University of Petroleum and Minerals, Dhahran, Saudi Arabia*

Keywords: Broadband Lasers, Quantum-Dot Lasers, Quantum-Dash Laser, Spectral Characteristics.

Abstract: We investigate the temperature dependent spectral characteristics of an InAs multi-stacked quantum-dash-in-well laser. The multi-stack active medium optical transitions are dispersed by varying the thickness of AlGaInAs barrier layers. The analysis is carried out via a Fabry-Perot 700 µm long-cavity laser with a ridge width of 2 µm at different temperatures. A lasing bandwidth of >40 nm is observed at room temperature with total optical power of >150 mW. Moreover, broadening of lasing spectrum is observed with increasing the temperature, due possibly to a thermionic assisted emission and to optical pumping, enabling a full exploitation of the inhomogeneous optical transitions within the active region which indicates an increase in the available states in the active region. Therefore, proper optimization of the multi-stack active medium is required to fully utilize these optical transitions while maintaining high quantum efficiency, and proper bandgap engineering the device structure.

## 1 INTRODUCTION

Due to several advantageous features of self-assembled quantum dash (Qdash) structures, they have become a focus of research and investigation in the past few years (Khan et al., 2013; Khan et al., 2014; Chen et al., 2002). Among the top of said features is the extraordinarily broad emission displayed by structures such as chirped InP-based InAs Qdash structures that can be exploited in several applications such as tenable sources, sensing, and optical communications (Khan et al., 2013; Khan et al., 2014). Given proper engineering and optimization, a single broadly emitting source can replace several combined traditional sources making for a great replacement that is eco-friendly and cost-efficient. However, what we lack in knowledge in the active medium of these structures and the involved quantum processes, that take place during emission, outweighs what we know. In order to fully exploit the potential of these these structures, optimization and characterization of different factors that affect their performance become more and more significant. It comes with no surprise that temperature is a prime factor as it plays a significant role in the non-uniform carriers' distribution and transition processes that take place within the active media of Qdash lasers. In this work, we characterize the temperature-dependent lasing spectral characteristics of a chirped multi-stacked InAs/InP Qdash laser and highlight the physics behind the emission profiles.

## 2 EXPERIMENT

The investigated laser diode in this work is a ridge-waveguide 2×700 µm$^2$ Fabry-Perot (FP) laser diode. The structure of its active medium is a chirped multi-stacked quantum-dash-in-well structure. Figure 1 illustrates the different layers within the chirped active medium. As Figure 1 shows, this structure is

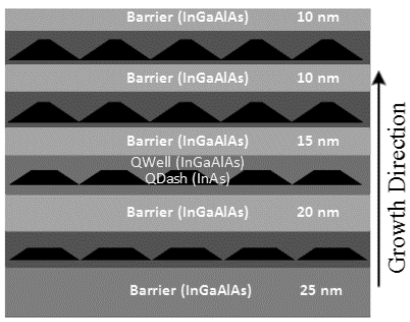


Figure 1: An illustration of the chirped active region of the multi-stacked quantum-dash-in-well structure.



Alkhazraji E., Khan M. and Khan M.
Broadband Lasing Characteristics of a Chirped InAs/InP Quantum-Dash Laser.
DOI: 10.5220/0006153502520255
In *Proceedings of the 5th International Conference on Photonics, Optics and Laser Technology (PHOTOPTICS 2017)*, pages 252-255
ISBN: 978-989-758-223-3

composed of four stacks of $In_{0.64}Ga_{0.16}Al_{0.2}As$ non-symmetrical 7.6 nm thick quantum-well layers. Within each layer are embedded five mono-layers of InAs quantum-dashes. Moreover, on top of each of the four stacks lies a tensile-strained $In_{0.50}Ga_{0.32}Al_{0.18}As$ barrier-layer. The thickness of the barrier layers has been shown in previous reports (Chen et al., 2002; Li et al., 2015) to play a significant role in controlling the size of the grown Qdashes and their corresponding emission. Thus, in order to increase the inhomogeneity of the active medium of the structure, the thickness of these of barrier-layers are varied from one layer to another as 20, 15, 10, and 10 nm. It has been found that Qdashes associated with wider barrier layers have a lower average height when compared to narrower barrier layers. A more detailed description of this structure can be found elsewhere (Khan et al., 2013).

For the sake of convenience, we shall denote each Qdash stack by its top barrier layer as S20, S15, S10a, and S10b while the last two combined shall be represented as S10 as a single group. Due to their varying thickness values, each stack can be associated with a separate ground state in addition to overlapping tail states with the neighbouring stacks.

We investigated the temperature-dependent lasing spectral profiles of the FP laser diodes by mounting them over a temperature controlled brass base while injecting them under a short pulse operation of a 0.2% duty cycle and a 0.5 µs pulse width. Thereafter, the lasing spectra have been obtained at different current injections. While operating under such low duty cycle (0.2%), it is safe to assume that the junction temperature of the laser diode is almost equal to that of the temperature-controlled brass base.

## 3 RESULTS AND DISCUSSION

Figure 2 (a) shows the L-I characteristic curves of this laser device at different temperatures, namely 15°C, 20°C (room temperature), 30°C, and 40°C, whereas Figure 2 (b) illustrates the energy-band diagram of the different stacks within the chirped active medium of the laser diode in addition to the overlapping density of states between adjacent Qdash stacks. Figure 1 (a) indicates that increasing the temperature of the laser device results in increasing its threshold current and decreasing the slope efficiency, particularly for higher values of injected current under high temperature values, as a result of the excess losses.

Figures 3 (a)–(d) show the lasing spectral profiles of the laser device under temperature values of 15°C, 20°C, 30°C, and, 40°C, respectively at different

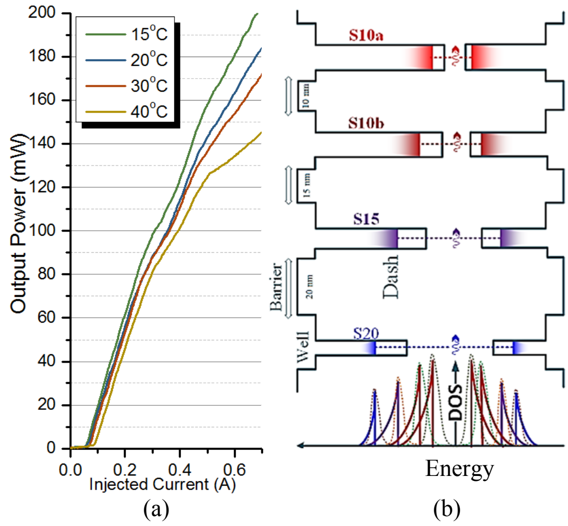


Figure 2: (a) The L-I characteristics of the laser diode at different temperatures. (b) The energy-band diagram of the chirped multi-stacked active medium alongside the corresponding overlapping zero-dimensional density of states.

injection current values starting from $1I_{th}$ and then sweeping between $1.2I_{th}$ and $7.6I_{th}$ in steps of $0.8I_{th}$. At low current injections, ($3.6I_{th}$ and lower), a single emission lobe begins to emerge around 1616 nm (shaded in green). Among the different stacks inside the active medium of this device, this initial emission can be attributed to the Qdashes within the stack associated with the intermediate barrier layer thickness and, consequently, the intermediate Qdash height which is the S15 stack. This attribution is based on the appreciable overlap of the ground state of that stack with tails of the neighbouring S20 and S10 stacks. Hence, Qdashes of the average intermediate height are expected to be the first to collectively achieve population inversion and initialize the lasing process.

Moreover, as we increase the pumped current, more Qdashes within the S15 stack and Qdashes within the overlapped tails from the neighbouring stacks are enabled to overcome the medium losses which ultimately leads to broadening the emission. However, this takes place at the expense a small red-shift in the emission due to the small bandgap shrinkage when the current is increased.

Nonetheless, when the injected current reaches $4.4I_{th}$, two side-lobes appear at both sides of middle main lobe which we shortly attributed to the S15 stack. Since Qdashes within the S10 stacks are generally of relatively larger heights, their emission components are expected to be higher in terms of

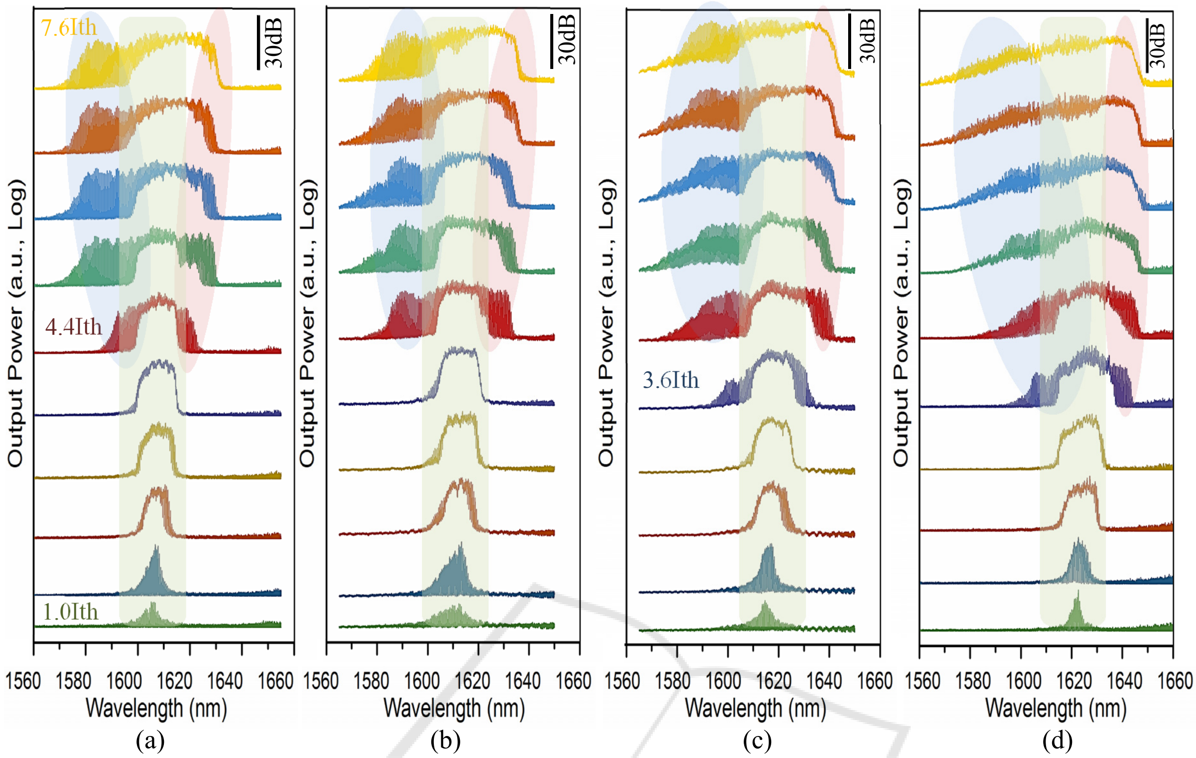


Figure 3: The lasing spectra of chirped Qdash ridge under different current injections (1.0 Ith, 1.2 – 7.6 Ith in steps of 0.8 Ith) at different temperatures of (a) 15°C, (b) 20°C, (c) 30°C, and (d) 40°C.

energy when compared to the shorter Qdashes within the S20 stack. In other words, the emission side lobe of the shorter wavelengths components (shaded in blue) can be attributed to the S20 stack while the longer wavelength lobe (shaded in red) can be associated with the narrow S10 Qdash stack. Nonetheless, with more current being injected, these side-lobes begin to merge with the main lobe into a single lobe possibly due to phono-assisted tunnelling that can be accelerated by high temperature values (Jiang and Singh, 1999). Furthermore, when comparing the progressive spectra of the low temperature case of 15° C with higher temperatures, it is worthy to note that a slower progressive spectrum broadening takes place at the lower temperature value. This is evident by the late appearance of the emission side lobes that only appear at current injections of 4.4 $I_{th}$ and beyond in the case of 15° C and 20° C while they emerge at earlier current injections of 3.6 $I_{th}$ in the case of 30° and 40° C.

These observations can be possibly explained by the increase in the junction temperature by directly increasing the temperature or due to the indirect temperature increase that results from the higher influx of carriers with higher current which results in increasing the number of Qdashes that can overcome the medium losses due the thermionic assisted emission that leads to increasing the density of carriers (Kittel, 1966). This, also, explains why this merging becomes more apparent as the temperature is increased as observed in Figure 3 (d) when compared to Figure 3 (a).

Moreover, this thermionic emission assistance becomes more evident when comparing the total emission 3dB bandwidth under the different temperature cases as it gets wider as the temperature is increased. For instance, Figure 3 (a) indicates that the 3 dB bandwidth is ~ 44 nm at a current injection of 7.6$I_{th}$. However, this bandwidth increases to ~ 48, 51, and 52 nm as the temperature is increased to 20° C, 30° C and 40° C, as shown in Figures 3 (b) – (d) respectively.

In other words, for any given injection current value, increasing the temperature aids the Qdashes within the tails of S20 and S10 stacks in achieving population inversion via the externally acquired thermal energy. Consequently, this enables more Qdashes within these stacks to overcome medium losses which introduces more emission wavelength components which, in turn, broadens the overall emission.

Ultimately, the variant average heights of each Qdash stack in addition to the individual height variance within the stack, both contribute to increasing the structure's inhomogeneity and introducing dissimilar emission components that add up to broaden the overall emission spectrum of the device.

Nevertheless, this broadening occurs at the expense of a reduction in the spectral power density of the device which translates to the progressive reduction in slopes in Figure 2 (a) as the temperature is increased which indicates a quenching in the quantum efficiency. Furthermore, this quench is evident by the signal-to-noise ratio (SNR) of this device of ~ 27 dB under 15$^o$ C when compared with the ~ 25 dB SNR at room temperature that is reduced even further at higher temperatures of 30$^o$ C and 40$^o$ C as it reaches ~ 23 dB and ~ 19 dB for both temperatures, respectively. Interestingly enough, this quenching effect is more apparent in the short wavelength (high energy) region of the lasing spectra which corresponds to the S20 stack and the high energy tails of S15 stack.

Previously in this work, we have suggested that the excess thermal energy that results from increasing the temperature plays a significant role in thermionically assisting the emission. However, this excess of thermal energy, in this case, results in carrier leakage when acquired by carriers within dashes of high energy states within the S20 stack and high energy tails of the S15 stack, which are more shallowly confined when compared to carriers within other Qdashes. Consequently, this results in a higher probability of carriers escaping from the potential confinement of these Qdashes since they can easily exhibit a thermally induced carrier spill-over due to their shallow quantum confinement.

# 4 CONCLUSIONS

With all said and done, this work provides a direct evidence to the effect of temperature on the non-uniform carrier dynamics and, in turn, the lasing spectral characteristics of the emission of the chirped InAs/InP Qdash structure. The rise in the junction that takes place with increasing the temperature directly or indirectly, via higher current injections, introduces a thermionic emission assistance that results in broadening the emission spectrum as more optical transitions become available. Nevertheless, this broadening occurs at the expense of deteriorating the quantum efficiency of the laser as a result of the thermally induced carrier leakage, particularly in the case of small-offset Qdash stacks. In other words, optimizing the structure of the active medium of the chirped multi-stacked laser is necessary in order to balance out this trade-off by minimizing the medium losses and by optimally utilizing these optical transitions while maintaining a high quantum efficiency.

# ACKNOWLEDGMENT

The authors thank King Fahd University of Petroleum and Minerals for the financial support through SR141002 grant.

# REFERENCES

M. Z. M. Khan, T. K. Ng, C.-S. Lee, P. Bhattacharya, and B. S. Ooi, *Effect of optical waveguiding mechanism on the lasing action of chirped* InAs/AlGaInAs/InP quantum dash lasers, in *Proc. SPIE, 2013*, pp. 86400.

M. Z. M. Khan, T. K. Ng, Lee, C. S., Bhattacharya, P., & Ooi, B. S. (2014). Investigation of chirped InAs/InGaAlAs/InP quantum dash lasers as broadband emitters. *IEEE Journal of Quantum Electronics*, 50(2), 51-61.

J. X. Chen, A. Markus, A. Fiore, U. Oesterle, R. P. Stanley, J. F. Carlin, et al.., "Tuning InAs/GaAs quantum dot properties under Stranski-Krastanov growth mode for 1.3 μm applications," *J. Appl. Phys.*, vol. 91, no. 10, pp. 6710–6716, 2002.

Li, S. G., Gong, Q., Cao, C. F., Wang, X. Z., Yan, J. Y., & Wang, Y. (2015). Thermal coefficient of InP-based quantum dot laser from cavity-mode measurements. *Infrared Physics & Technology*, 68, 119-123.

Jiang, H., & Singh, J. (1999). Nonequilibrium distribution in quantum dots lasers and influence on laser spectral output. *Journal of applied physics*, 85(10), 7438-7442.

Kittel, Charles. *Introduction to solid state.* John Wiley & Sons, 1966.